

Article

A Case of Interdisciplinary Fusion under Dual Carbon Goal: Coordinated Carbon Reduction with Greenhouse Photovoltaics and Electric Vehicles

Juai Wu ¹, Shiyang Deng ¹, Yuanmeng Zhu ¹, Yun Liu ², Yang Andrew Wu ³, Rong Fu ^{1,*} and Sipeng Hao ^{2,*}

¹ College of Automation & College of Artificial Intelligence, Nanjing University of Posts and Telecommunications, Nanjing 210023, China

² School of Electric Power Engineering, Nanjing Institute of Technology, Nanjing 211167, China

³ Division of Science, Engineering and Health Studies, College of Professional and Continuing Education, The Hong Kong Polytechnic University, Hong Kong

* Correspondence: furong@njupt.edu.cn (R.F.); j00000000833@njit.edu.cn (S.H.)

Abstract: Building a new type of power system is an important guarantee to support China's "dual carbon" goal. Due to the inseparable relationship between industrial and agricultural production and electric energy utilization, there must be interdisciplinary integration to achieve the goal of "dual carbon". The disciplines of horticulture and electric power are taken as examples in this paper to analyze the feasibility of carbon emission reduction through coordinating agricultural photovoltaic (PV) greenhouse and electric vehicle (EV) energy storage. Firstly, the mechanism of carbon emission difference caused by electric energy supplementing during EV charging is analyzed. Secondly, in the context of the contradiction between the reduction of battery life caused by discharging (increasing carbon emission) and the increase in PV output consumption by orderly charging and discharging (reducing carbon emission), an optimization model for the synergistic operation of EV clusters and greenhouse PVs (with the objective of minimizing carbon emissions) is proposed. Finally, the effectiveness of the proposed model is verified through simulation cases. The energy storage characteristics of EVs is capable of realizing the transfer of PV power generation in the time dimension, and the coordinated operation of greenhouse PVs and EVs' charging and discharging can effectively reduce carbon emission during the EV operation period. In a typical summer scenario of PV output, the carbon emission of EVs in V2G (vehicle to grid) mode was reduced by 69.13% compared to disorderly charging. It is shown that the adequacy of PV generation and the orderly dispatching of the charging and discharging of EVs are the key factors in reducing carbon emission throughout the life cycle of EVs.

Keywords: carbon emission; electric vehicle; photovoltaic greenhouse; battery life; interdisciplinary integration



Citation: Wu, J.; Deng, S.; Zhu, Y.; Liu, Y.; Wu, Y.A.; Fu, R.; Hao, S. A Case of Interdisciplinary Fusion under Dual Carbon Goal: Coordinated Carbon Reduction with Greenhouse Photovoltaics and Electric Vehicles. *Appl. Sci.* **2023**, *13*, 2410. <https://doi.org/10.3390/app13042410>

Academic Editor: Jingyang Fang

Received: 17 January 2023

Revised: 7 February 2023

Accepted: 10 February 2023

Published: 13 February 2023



Copyright: © 2023 by the authors. Licensee MDPI, Basel, Switzerland. This article is an open access article distributed under the terms and conditions of the Creative Commons Attribution (CC BY) license (<https://creativecommons.org/licenses/by/4.0/>).

1. Introduction

In response to climate change and to meet the Paris Agreement's goal of keeping temperatures within 2 °C, many countries have set clear timelines for carbon peaking and carbon neutrality [1,2]. China has proposed a national strategic goal of "carbon peaking by 2030 and carbon neutrality by 2060" ("dual carbon" goal). In the energy field, the use of fossil fuels is the main source of global carbon emission [3,4]. As a relatively mature technology that can replace oil-fueled vehicles, the potential of electric vehicles (EVs) in reducing carbon emission and exhaust pollution has gradually emerged [5–7]. In the agricultural field, as a basic industry to ensure national food security and ecological security, its high-quality development is also of great significance to the realization of the "dual carbon" goal. Agriculture is a typical artificial ecosystem that involves energy consumption in many of its links, such as production, storage and transportation. Therefore,

it is necessary to coordinate the development of the energy field and agriculture field under the “dual carbon” goal.

Compared with coal-fired power units and gas turbine units, photovoltaic (PV) power generation has significant carbon emission reduction benefits. PV is also of great significance to agricultural development. The governance mode of the combination of PV and water harvesting irrigation has not only the function of ecological restoration but also the economic benefits of agricultural production [8–10]. Greenhouse planting is a typical method for the intensive production of agricultural products [11]. Greenhouse PV can not only save land resources, but also increase the output efficiency per unit area of land [12]. If greenhouse PV power generation is used as the power source during the EV operation, it will play a positive role in the carbon reduction throughout the life cycle of the EV.

In the existing research regarding the orderly dispatching of EVs, revenue is generally taken as the optimization objective [13]. An optimization strategy for EVs’ participation in the frequency management market, with the goal of maximizing the revenue of EVs, was proposed in [14]. Research on the day-ahead scheduling optimization of the microgrid with the goal of minimizing the operating cost of the microgrid was carried out in [15]. A multi-objective EV-charging optimization model considering power purchase costs and battery cycle capacity was constructed in [16]. However, the studies on EV charging and discharging scheduling strategies for life cycle carbon emission and multi-field coordination between EV and other industry fields are rarely involved [17]. There is a random and fluctuating nature in greenhouse PV output, and although the time mismatch between PVs and EVs in terms of power replenishment can be resolved by deploying energy storage plants, it also faces the problem of high cost [18,19]. EVs are purchased by individual users without additional energy storage purchase costs. The high cost of energy storage power plants can be addressed by using EVs to participate in V2G (vehicle to grid) [20,21]. However, V2G will increase the losses to the battery and shorten its life [22]; thus, it is necessary to sign compensation contracts between EV users and EV aggregators to solve the problem of EV users’ willingness to accept orderly charging and discharging [23,24].

Based on the above analysis, the energy supply synergy between EVs and agricultural greenhouse PV power plants in reducing the carbon emission of EVs throughout its life cycle is taken as the research object in this paper. The remainder of the paper is organized as follows. In Section 2, the sources of carbon emission in the EV life cycle are analyzed. In Section 3, based on the dynamic battery life decay model considering internal resistance growth and capacity decay, a coordinated scheduling optimization model of EVs and PV power plants aimed at minimizing carbon emission is constructed. Section 4 proposes a solution method for the scheduling optimization model. In Section 5, the effectiveness of the proposed model is verified by using simulation cases. The significance of this study and some conclusions are concluded in Section 6.

2. The Carbon Emission throughout the EV Life Cycle

Life cycle assessment refers to the technical method of compiling and evaluating the relevant inputs, outputs and their potential impacts throughout the whole life cycle of a product system [25]. Among them, Life Cycle Inventory Analysis (LCIA) is a process of quantifying waste emission and resource consumption throughout the entire life cycle, and it is one of the most critical segments in product life cycle evaluation. The accuracy of the data will directly affect the final evaluation result.

Therefore, under the vision of “dual carbon”, countries around the world are promoting the large-scale application of EVs. The full life cycle of an EV is divided into three stages: production, operation and recycling. Among them, the production stage is subdivided into raw material manufacturing and assembly; the operation stage includes the use of electrical energy, operation and maintenance; the recycling stage is the recycling of recyclable materials and the processing of non-recyclable materials. The system boundaries of the three stages and their life cycle lists are shown in Figure 1.

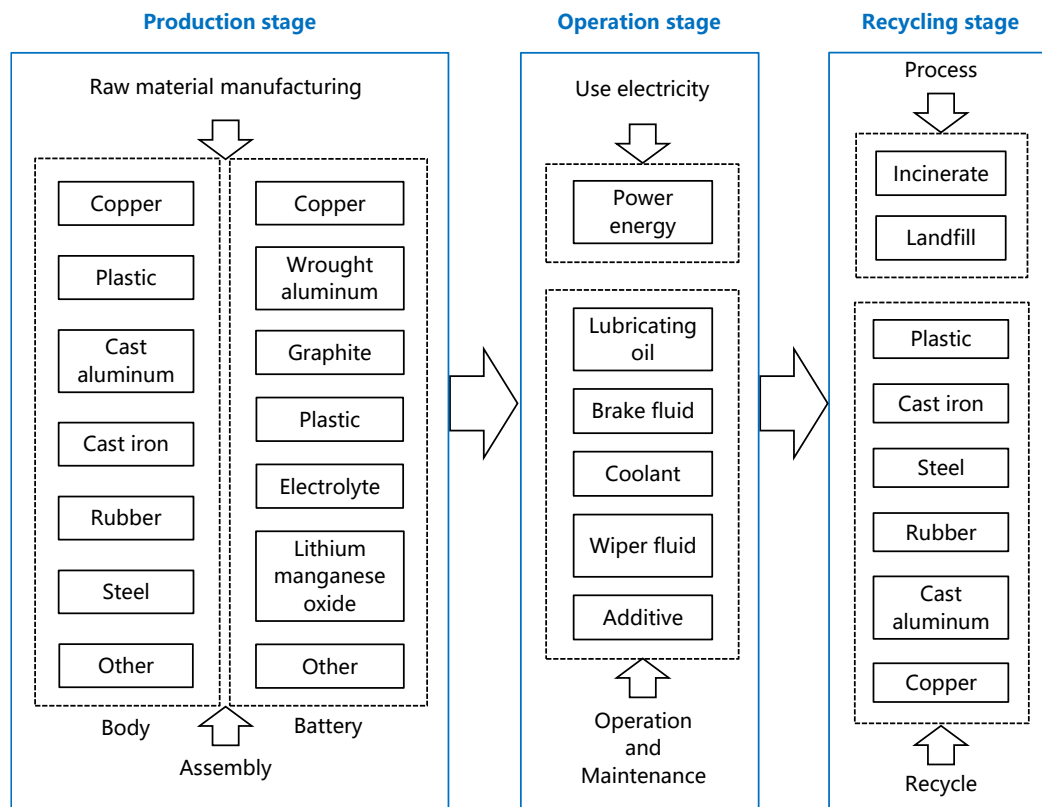


Figure 1. Boundary graph of the whole life system of EVs.

During the entire life cycle of an EV, carbon emission mainly comes from the manufacturing of power batteries in the production stage and the use of electric power in the operation stage. It is pointed out in [26] that the variability of the power supply structure has a great impact on the life-cycle carbon reduction of EVs, wherein the higher the proportion of clean energy generation, the lower the life-cycle carbon emission of EVs compared to oil-fueled vehicles.

EVs and oil-fueled vehicles of the same quality were selected to calculate the carbon emission of the whole life cycle (as shown in Table 1) [27], and the analysis showed that the source of electricity during the EV operation stage was the major factor triggering the difference in EV carbon emission.

Table 1. Calculation of carbon emission during the entire life cycle of different types of vehicles.

Type of Vehicle	Production Stage /kg	Operation Stage /kg	Recycling Stage /kg	Total /kg
EV (supplied with coal electricity)	12,525.8	66,232.4	−1495.8	77,262.4
EV (supplied with clean energy)	12,525.8	6832.4	−1495.8	17,862.4
Oil-fueled vehicle	13,800.3	50,342.3	−2604.1	61,538.5

3. Co-Optimization Model of EVs and PVs

A photovoltaic greenhouse is a typical “photovoltaic + agriculture” mode. It is a cover installed on the roof of a greenhouse, and although the photovoltaic panels can block sunlight and affect the normal growth of crops to a certain extent, they are arranged in a chessboard shape (as shown in Figure 2). This is more suitable for the growth of crops compared to a linear shape arrangement, and it can realize a good combination of photovoltaic power generation and greenhouse crop growth [28].

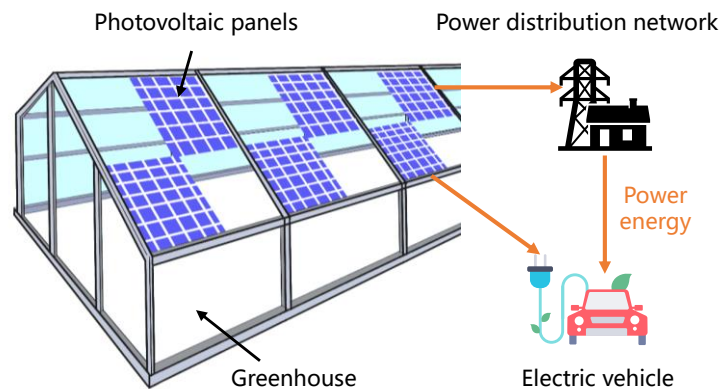


Figure 2. Schematic diagram of cooperative operation of EVs and greenhouse PVs.

In the process of coordinated operation of EVs and agricultural greenhouse PV power plants, it is necessary to increase the consumption of PV power generation as much as possible in order to reduce carbon emission (Figure 2). Due to the uncertainty of PV output, it is inevitably required to charge and discharge EVs cyclically, but this further increases the loss of battery life. Therefore, both the reduction in carbon emission due to the increased PV consumption and the increase in carbon emission due to battery life loss caused by discharge need to be quantitatively analyzed during the collaborative optimization.

3.1. Objective Function

Ignoring the carbon emissions caused by the loss of fluids (oil, coolant, and lubricating oil) for operation and maintenance when the EV runs, we take a scheduling cycle T as an example and construct an optimization model with the objective of minimizing carbon emission, which is shown in Equation (1).

$$\min C = \sum_{i=1}^N c_{ev.lifelos}^i + c_{ev.grid} \quad (1)$$

where C is the total carbon emission during the charging process; N is the total number of EVs; $c_{ev.lifelos}^i$ is the carbon emission equivalent to the battery life loss during the charging and discharging process of the i th EV; and $c_{ev.grid}$ is the carbon emission when the EV cluster is charged directly from the power grid.

By discretizing the time axis, dividing a scheduling cycle into n periods of length Δt ($\Delta t = T/n$), and freezing the time-varying EV charging and discharging power in the period of Δt , Equation (1) can be decomposed into Equation (2).

$$\min C = \sum_{i=1}^N \sum_{k=1}^{T/\Delta t} c_{ev.lifelos}^i(k) + \sum_{k=1}^{T/\Delta t} c_{ev.grid}(k) \quad (2)$$

Thereinto,

$$c_{ev.grid}(k) = \lambda_{grid} \left(\sum_{i=1}^N P_{ev}^i(k) - P_{ev.pv}(k) \right) \Delta t \quad (3)$$

$$c_{ev.lifelos}^i(k) = \lambda_{battery} / M^i \left(D^i(k), SOC^i(k) \right) \quad (4)$$

where λ_{grid} is the carbon emission factor of grid power generation; $P_{ev}^i(k)$ is the charging and discharging power of the EV in the k period, which is greater than 0 when charging and less than 0 when discharging (when $P_{ev}^i(k) < 0$, $P_{ev}^i(k) = P_{ev.discharge}^i(k)$); $P_{ev.pv}(k)$ is the total power supplied to EVs from PV power plants in period k ; $\lambda_{battery}$ is the carbon emission coefficient of the EV power battery life cycle; and M is the battery cycle life (the total number of battery cycles), which is related to the discharge depth D and the SOC

(state of charge) of the battery during discharge, i.e., $1/M^i$ is the life loss of the battery in a single discharge cycle.

3.2. Battery Life Loss Model

The aging mechanism of the battery itself is mainly the formation of a Solid Electrolyte Interphase (SEI) on the contact surface of the battery's negative electrode and the electrolyte, which consumes the active material and reduces the battery capacity. Generally, when the battery capacity decays to 80% of the initial capacity, it is considered that the battery life has reached the end of its battery life cycle. Additionally, the battery cathode will also structurally age under the action of various mechanisms. In addition to its own physical characteristics, the aging process of the battery is affected by environmental factors such as state of charge, depth of discharge, temperature and humidity.

The battery life model is mainly divided into the mechanism model and the external characteristic model. The mechanism model is modeled according to the physical and chemical reactions inside the battery. It has high accuracy but is complex, which is not conducive to the calculation of the simulation model. The external characteristic model is based on a data-driven method, using experimental data to model the battery life by observing the capacity fade and internal resistance growth exhibited during cycling [29,30].

Differentiating from the battery loss model that only combines the depth of discharge, a half-empirical and half-mechanical dynamic battery life decay model that combines the internal resistance growth model with the capacity decay model was used, as shown in Equation (5), which takes into account environmental factors such as the depth of discharge, battery SOC and temperature [31].

$$M^i(k) = \frac{Q_{site}}{c_{ref}T_{acc}} \left(\frac{D^i(k)}{D_{ref}} \right)^{-\beta} e^{-\frac{\alpha F}{R}(SOC^i(k) - SOC_{ref})} \quad (5)$$

The depth of discharge D is defined as the difference between the load state at the beginning of the discharge and the load state at the end of the discharge. The formalization of the depth of discharge of the i th EV is shown in Equation (6); the initial state of SOC^i of the i th EV is formalized, as shown in Equation (7).

$$D^i(k) = \frac{\left| \sum_{k_{discharge.start}^i}^{k_{discharge.end}^i} P_{ev.discharge}^i(k) \Delta t \right|}{E_{max}} \quad (6)$$

$$SOC^i(k) = \frac{E^i(k)}{E_{max}} \quad (7)$$

$$E^i(k) = E_{start}^i + \sum_{k_{start}^i}^k P_{ev}^i(k) \Delta t \quad (8)$$

In Equations (5)–(8), Q_{site} is the capacity decay rate; T_{acc} is the temperature acceleration coefficient; D_{ref} is the standard depth of discharge; SOC_{ref} is the standard value of the state of charge at the beginning of the discharge cycle; F is the Faraday constant; R is the molar gas constant; α , β , and c_{ref} are fitting constants, which can be obtained by fitting the experimental data of the battery; E_{max} is the battery capacity; E^i is the current capacity of the i th EV battery; $k_{discharge.start}^i$ is the start time of a period of discharge; and $k_{discharge.end}^i$ is the end time of a period of discharge.

3.3. Constraints

(1) Battery power constraints

In order to meet the uncertain travel needs of EV users, the electric quantity of an EV shall not be lower than the minimum electric quantity E_{ms} at all times, in addition to

reaching the expected electric quantity of users when off grid. If the electric quantity of an EV is lower than E_{ms} when connected to the power grid, it should be charged to the minimum electric quantity at the maximum power immediately after being connected to the power grid [32].

Therefore, according to the difference of the initial electric quantity E_{start} when the EV is connected to the power grid, the formalization of the EV battery electric quantity constraint is shown in Equations (9) and (10).

① when $E_{start}^i < E_{ms}^i$

$$E_{min}^i(k) = \begin{cases} E_{start}^i + P_{max}\Delta t(k - k_{start}^i), & k_{start}^i \leq k < k_{ms}^i \\ E_{ms}^i, & k_{ms}^i \leq k < \left[k_{end}^i - (E_{exp}^i - E_{ms}^i)/P_{max} \right] \\ E_{exp}^i - P_{max}\Delta t(k_{end}^i - k), & \left[k_{end}^i - (E_{exp}^i - E_{ms}^i)/P_{max} \right] \leq k \leq k_{end}^i \end{cases} \quad (9)$$

② when $E_{start}^i \geq E_{ms}^i$

$$E_{min}^i(k) = \begin{cases} E_{ms}^i, & k_{start}^i \leq k < \left[k_{end}^i - (E_{exp}^i - E_{ms}^i)/P_{max} \right] \\ E_{exp}^i - P_{max}\Delta t(k_{end}^i - k), & \left[k_{end}^i - (E_{exp}^i - E_{ms}^i)/P_{max} \right] \leq k \leq k_{end}^i \end{cases} \quad (10)$$

where $E_{min}^i(k)$ is the minimum electric quantity required to be satisfied by the i th EV in time period k ; E_{ms}^i is the guaranteed minimum electric quantity of the i th EV; E_{exp}^i is the expected electric quantity when the i th EV user is off the power grid; P_{max} is the maximum charge and discharge power of the EV; k_{start}^i is the time when the i th EV is connected to the power grid; k_{ms}^i is the time when the i th EV is charged to the guaranteed minimum electric quantity; and k_{end}^i is the time when the i th EV is off grid.

(2) Charge-discharge power constraints of a single EV

The upper and lower limit constraints of the charge and discharge power of the EV are shown in Equation (11). The values of the minimum charging power, the maximum charging power and the maximum discharging power in each time period are shown in Equations (12) and (13).

$$-P_{ev.min}^i(k) \leq P_{ev}^i(k) \leq P_{ev.max}^i(k) \quad (11)$$

$$P_{ev.max}^i(k) = \begin{cases} P_{max}(k), & P_{max}(k) \leq E_{max} - E^i(k) \\ E_{max} - E^i(k), & E_{max} - E^i(k) \leq P_{max}(k) \\ 0, & E_{max} - E^i(k) \leq 0 \end{cases} \quad (12)$$

$$P_{ev.min}^i(k) = \begin{cases} P_{max}(k), & P_{max}(k) \leq E^i(k) - E_{min}^i(k+1) \\ E^i(k) - E_{min}^i(k+1), & P_{max}(k) > E^i(k) - E_{min}^i(k+1) \\ 0, & E^i(k) - E_{min}^i(k+1) \leq 0 \end{cases} \quad (13)$$

(3) Total power constraints

The power supplied by the PV power plant to the EV cluster should be less than the total power generated by the PV power plant (as shown in Equation (14)). The charging power supplied by the power grid to the EV should not be less than 0 (as shown in Equation (15)).

$$P_{pv.sum}(k) \geq P_{ev.pv}(k) \quad (14)$$

$$P_{ev.grid}(k) \geq 0 \quad (15)$$

where $P_{pv.sum}(k)$ is the output of the PV power station in period k .

3.4. Optimization Model with EV Not Participating in Discharge

An EV not participating in discharge is a special case of the objective function in Section 3.1, in which Equation (2) can be rewritten as Equation (16). The constraints are Equations (9), (10), (12), (14), (15) and (17).

$$\min C = \sum_{k=1}^{T/\Delta t} \lambda_{grid} \left(\sum_{i=1}^N P_{ev}^i(k) - P_{ev,pv}(k) \right) \Delta t \quad (16)$$

$$P_{ev}^i(k) \geq 0 \quad (17)$$

4. Solution Process

In order to minimize the overall carbon emissions, it is necessary to increase the consumption of PV power generation as much as possible and use the stored PV power generation in EVs by discharging. Under this circumstance, it is required to compare the carbon emissions caused by the battery life loss when discharging with the carbon emissions when directly supplied by the distribution network. Through the simulation in MATLAB, it was found that for a given EV model, when the same amount of electricity is supplied, the carbon emission with a direct power supply from the distribution network is always greater than the carbon emission of the EV battery life loss. The comparison results of the simulation are shown in Figure 3.

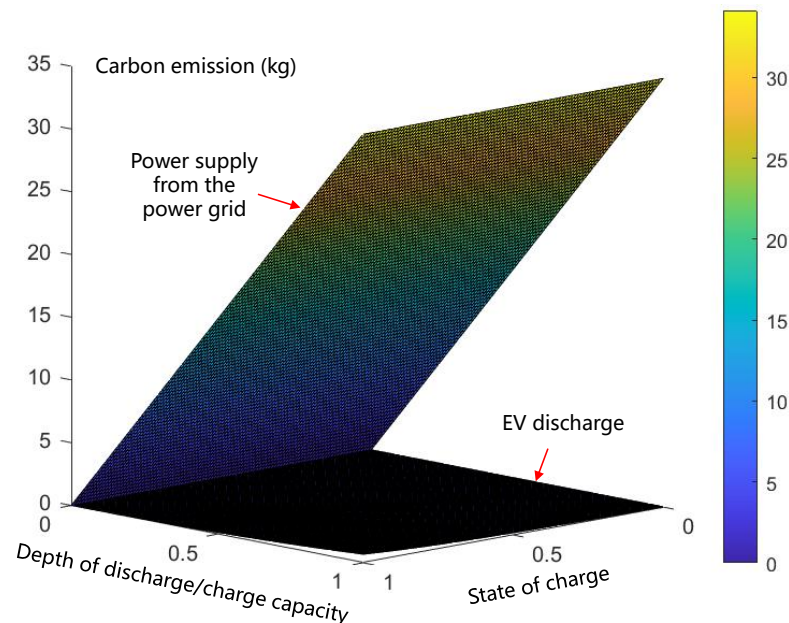


Figure 3. Comparison of battery discharging carbon emissions and distribution network carbon emissions.

Therefore, the optimization model can be linearized, and the objective function Equation (1) is simplified to the solution of Equation (18). The EV's charging and discharging strategies are the same when they are optimal. After the solution is completed, the carbon emissions equivalent to battery life loss are calculated according to the optimization results. The optimization flow is shown in Figure 4. The optimization solution process is implemented in the MATLAB simulation environment with the help of Yalmip and Gurobi optimization toolkits.

$$\min C' = c_{ev,grid} \quad (18)$$

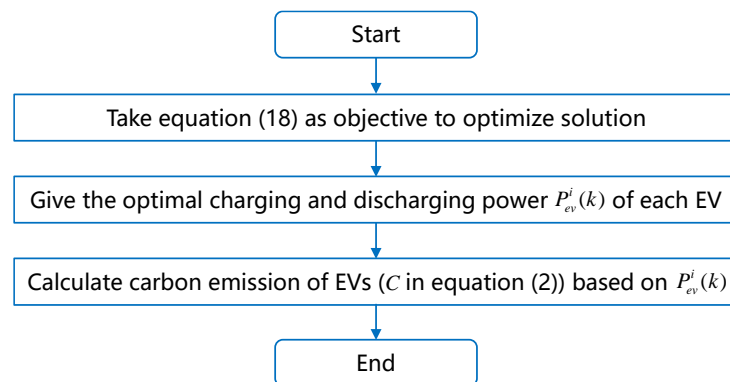


Figure 4. Optimization flow.

5. Case Analysis

5.1. Simulation Parameter Settings

For parameters related to battery life decay, take the capacity decay rate $Q_{site} = -0.2$; temperature acceleration coefficient $T_{acc} = 1$; standard depth of discharge $D_{ref} = 60\%$; standard value of state of charge at the beginning of discharge cycle $SOC_{ref} = 80\%$; $c_{ref} = -2.395 \times 10^{-5}$, $\alpha = 2.4106 \times 10^{-6}$, $\beta = 2.2227$; Faraday constant $F = 96,485.3383$; and molar gas constant $R = 8.3145 \text{ J}/(\text{mol} \cdot \text{K})$.

The carbon emission factor of the power generation of grid is $\lambda_{grid} = 0.69 \text{ kg}/\text{k} \cdot \text{Wh}$; the number of EVs is $N = 100$; the maximum battery power is $E_{max} = 50 \text{ kW} \cdot \text{h}$; the maximum charging and discharging power is $P_{max} = 6 \text{ kW}$; the guaranteed minimum power is $E_{ms} = 50\% E_{max}$; the user's expected power is $E_{exp} = 95\% E_{max}$ when off grid; $\Delta t = 1 \text{ h}$; the SOC of the EV when it is connected to the power grid obeys the uniform distribution of $[0.2, 0.8]$, and the starting time of the grid connection obeys the uniform distribution; the grid connection duration is 12 h. Suppose the module area of the PV power station is 3000 m^2 , the module parameters are 300 WP, and the output of the PV power station $P_{pv.sum}(k)$ is given by the Pvsyst 7.2 simulation software [33,34].

The main source of life-cycle carbon emission of an EV battery is raw material manufacturing, which is 2093.43 kg in total; the emission reduction benefit of battery recycling is 50%; therefore, the total carbon emissions in the battery life cycle is 1046.72 kg, which is used as the basis for estimating the carbon emissions caused by the reduction of battery life [27,35].

5.2. Simulation Case Settings

The output data of agricultural greenhouse PV power plants (as shown in Figure 5) were selected for comparison and analysis under the typical winter scenario (daily average output in January) and the typical summer scenario (daily average output in July). The specific simulation case settings are shown in Table 2, in which “disorderly charging” means that EVs are charged to the users' expected power immediately after connected to the power grid, “G2V” means orderly charging (discharging is not supported), and “V2G” means orderly charging (discharging is supported).

Table 2. Simulation cases.

Case Number	Authority of EV Scheduling	Scenario of PV Output
1	Disorderly charging	Typical scenario in winter
2	G2V	
3	V2G	
4	Disorderly charging	Typical scenario in summer
5	G2V	
6	V2G	

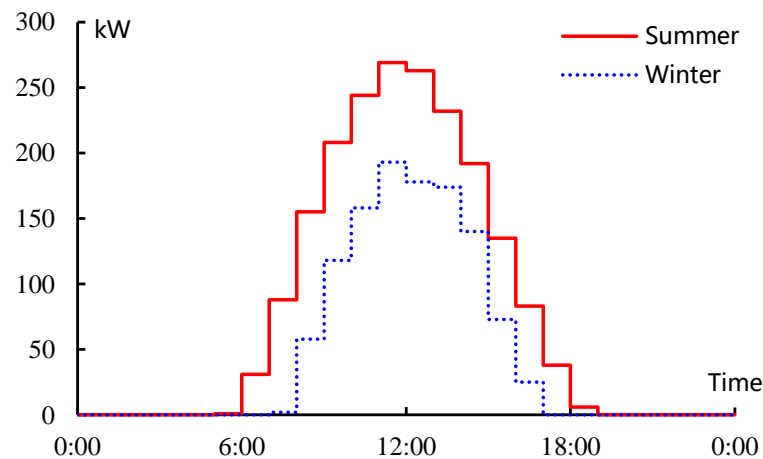


Figure 5. PV power generation in winter and summer (hourly average).

5.3. Result Analysis

Combined with the above parameter settings, it is easy to know that the total power demand of the EV cluster is 2194.00 kW·h.

5.3.1. Typical Scenario in Winter

The PV output curve under this scenario is shown in Figure 6, and the total PV power generation is 1119.00 kW·h. It can be seen from the power curves of EV clusters in the different cases that due to the low PV output in winter, all PV power generation is used for EV charging in case 2 and 3 of orderly EV charging. The carbon emissions of EV charging and discharging in each case are shown in Table 3.

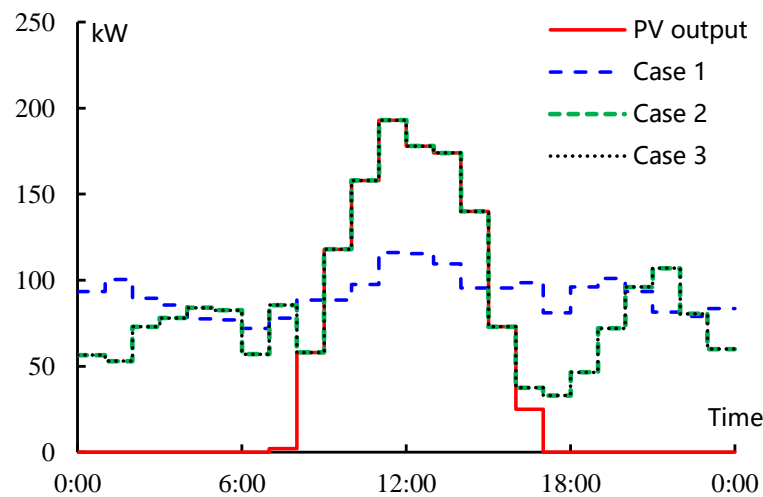


Figure 6. Power curves of EV clusters in typical winter scenario.

Table 3. Carbon emissions of EV charging and discharging in different cases.

Case Number	PV Power Obtained by EVs/k·Wh	EVs Carbon Emissions/kg	Total PV Power Generation/k·Wh
1	780.50	975.32	1119.00
2	1119.00	741.75	
3	1119.00	741.75	
4	1043.50	793.85	1945.00
5	1585.00	420.21	
6	1839.50	245.06	

5.3.2. Typical Scenario in Summer

In this scenario, the total PV power generation is 1945.00 kW·h. From the power curves of EV clusters in the different cases in Figure 7, it can be seen that when the PV power generation is sufficient, the orderly charging of the EVs that support discharging will significantly promote the consumption of PV power generation. In Table 3, compared with the disorderly charging in case 4, the carbon emissions in case 5 and case 6 are reduced by 47.03% and 69.13%, respectively.

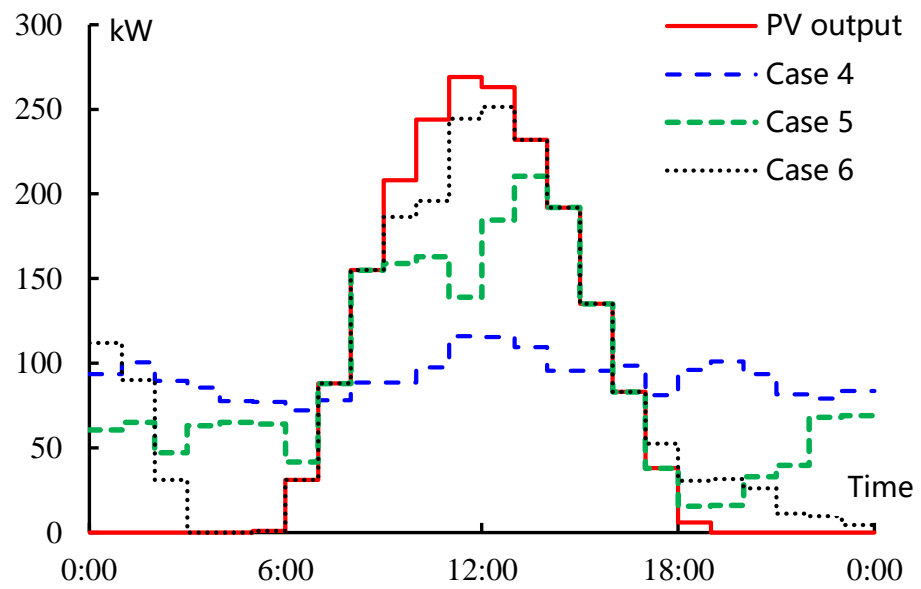


Figure 7. Power curves of EV clusters in typical summer scenario.

5.4. Uncertainty Analysis of PV Output

Affected by the random fluctuation of weather, the output of greenhouse PV is essentially uncertain, and the risk optimization of the EV charging and discharging strategy can be realized by the scenario analysis method [36]. Therefore, the objective function of Equation (2) is transformed into Equation (19), where ρ_s is the probability of PV output scenario s .

$$\min C = \sum_{s \in S} \rho_s \left(\sum_{i=1}^N \sum_{k=1}^{T/\Delta t} c_{ev.lifeloss}^i(k) + \sum_{k=1}^{T/\Delta t} c_{ev.grid}(k) \right) \quad (19)$$

Taking $[0, 1]$ as the interval, the occurrence probability of a typical winter scenario is gradually perturbed with the step of 0.1, and the sum of the occurrence probabilities of typical scenarios in winter and summer is 1. Figure 8 shows the carbon emissions of EV clusters under different scenario occurrence probabilities. With the increase in the probability of a typical winter scenario, the total PV power obtained by EV clusters will gradually decrease, which leads to an increasing trend of carbon emissions of EV clusters.

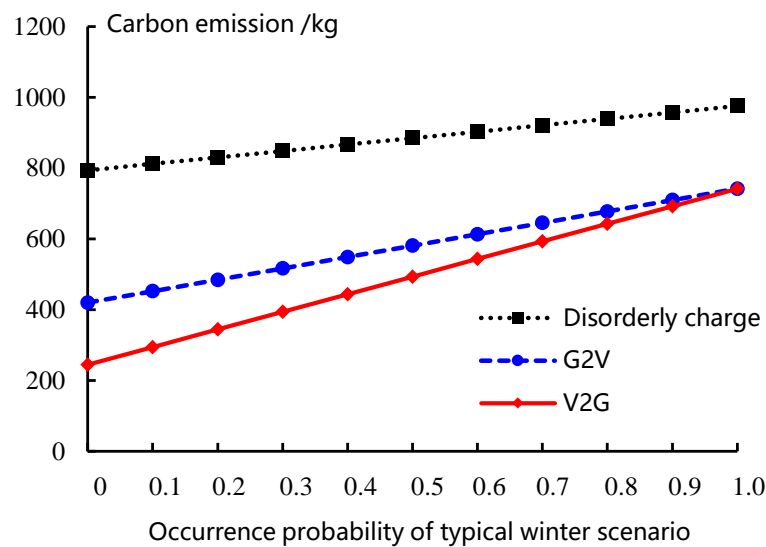


Figure 8. Carbon emission of EV clusters under uncertain scenarios.

6. Conclusions

Carbon emission reduction is a systematic project involving many fields, and it is extremely important to carry out cross-field interactive and collaborative research. This paper explored the feasibility of combining the fields of agriculture and energy for emission reduction. The carbon emission reduction benefits of EVs mainly depend on the power supply structure during operation. The proportion of low-carbon power in the charging process of EVs can be effectively increased by coordinating the EV clusters that have energy storage characteristics and the greenhouse PV outputs which have high volatility and randomness.

The mechanism of carbon emission changes caused by electric energy supplementation during EV operation was analyzed in this paper; battery life reduction caused by discharging, which will increase carbon emissions, and orderly charging and discharging can improve PV output consumption, which will reduce carbon emissions. An optimization model for the coordinated operation of EV clusters and agricultural greenhouse PVs was proposed with the goal of minimizing carbon emissions. The analysis of the simulation cases shows that the proposed optimization model effectively reduces carbon emissions during EV operation. The adequacy of PV output and the orderly charging and discharging scheduling of EVs are the key factors for reducing the carbon emissions of the whole life cycle of EVs. In the typical winter and summer scenarios of PV output, compared to disorderly charging, the carbon emissions of EVs in the V2G mode were reduced by 23.95% and 69.13%, respectively.

This study considered only the carbon emissions of EV operation, and did not integrate the greenhouse energy consumption process. The next step of research will be based on the coordinated operation of greenhouse PVs and EVs to further take into account the energy consumption in the growth process of greenhouse agricultural crops to maximize the overall benefit. Furthermore, in order to promote the practical application feasibility of the scheme proposed in this paper, the top-level design and some promotion policies for improving the interaction between EVs and distributed greenhouse PVs should be formulated. Some innovative business models and market mechanisms should be designed to increase the willingness of EV users and greenhouse PV users to participate in the interaction.

Author Contributions: Conceptualization, J.W. and S.H.; methodology, J.W.; software, S.D. and Y.Z.; validation, J.W. and Y.A.W.; formal analysis, S.D.; investigation, Y.Z.; resources, Y.L. and S.H.; data curation, S.D.; writing—original draft, J.W., S.D. and Y.L.; writing—review and editing, J.W. and R.F.; visualization, Y.Z.; supervision, Y.A.W.; project administration, S.H.; funding acquisition, J.W. and R.F. All authors have read and agreed to the published version of the manuscript.

Funding: This research was funded by (1) the Open Research Fund of Jiangsu Collaborative Innovation Center for Smart Distribution Network, Nanjing Institute of Technology, grant number XTCX202104, (2) the Education Reform Project of Nanjing University of Posts and Telecommunications (NO. JG00514JX56) and (3) the Research Grant Council of Hong Kong SAR, project reference number UGC/FDS24/E08/21.

Institutional Review Board Statement: Not applicable.

Informed Consent Statement: Not applicable.

Data Availability Statement: Not applicable.

Conflicts of Interest: The authors declare no conflict of interest.

Nomenclature

PV	Photovoltaic
EV	Electric vehicle
V2G	Vehicle to grid
T	Scheduling cycle
C	Total carbon emission
N	Total number of EVs
$c_{ev.lifeloss}^i$	Carbon emission equivalent to the battery life loss of the i th EV
$c_{ev.grid}$	Carbon emission when the EV is charged directly from power grid
Δt	Time length of each period
λ_{grid}	Carbon emission factor of grid power generation
$P_{ev}^i(k)$	Charging and discharging power of the EV in period k
$P_{ev.pv}(k)$	Total power supplied to EVs from PV power plants in period k
$\lambda_{battery}$	Carbon emission coefficient of the EV power battery life cycle
M	Total number of battery cycles
D	Discharge depth
SOC	State of charge
Q_{site}	Capacity decay rate
T_{acc}	Temperature acceleration coefficient
D_{ref}	Standard depth of discharge
SOC_{ref}	Standard value of the state of charge at the beginning of the discharge cycle
F	Faraday constant
R	Molar gas constant
α, β, c_{ref}	Battery fitting constants
E_{max}	Battery capacity
E^i	Current capacity of the i th EV battery
$k_{discharge.start}^i$	Start time of a period of discharge
$k_{discharge.end}^i$	End time of a period of discharge
$E_{min}^i(k)$	Minimum electric quantity required to be satisfied by the i th EV in time period k
E_{ms}^i	Guaranteed minimum electric quantity of the i th EV
E_{exp}^i	Expected electric quantity when the i th EV user is off the power grid
P_{max}	Maximum charge and discharge power of EV
k_{start}^i	The time when the i th EV is connected to the power grid
k_{ms}^i	The time when the i th EV is charged to the guaranteed minimum electric quantity
k_{end}^i	The time when the i th EV is off grid
$P_{pv.sum}(k)$	Output of the PV power station in period k
ρ_s	Probability of PV output scenario s

References

1. Meinshausen, M.; Lewis, J.; McGlade, C.; Gütschow, J.; Nicholls, Z.; Burdon, R.; Cozzi, L.; Hackmann, B. Realization of Paris Agreement pledges may limit warming just below 2 °C. *Nature* **2022**, *604*, 304–309. [[CrossRef](#)] [[PubMed](#)]
2. Hasan, M.M.; Wu, C.B. Estimating energy-related CO₂ emission growth in Bangladesh: The LMDI decomposition method approach. *Energy Strategy Rev.* **2020**, *32*, 100565. [[CrossRef](#)]

3. Mcglade, C.; Ekins, P. The geographical distribution of fossil fuels unused when limiting global warming to 2 °C. *Nature* **2015**, *517*, 187–190. [CrossRef] [PubMed]
4. Hasan, M.M.; Liu, K. Decomposition analysis of natural gas consumption in Bangladesh using an LMDI approach. *Energy Strategy Rev.* **2022**, *40*, 100724. [CrossRef]
5. Wu, J.A.; Wang, Z.Y.; Xu, T.H.; Sun, C.Y. Driving mode selection through SSVEP-based BCI and energy consumption analysis. *Sensors* **2022**, *22*, 5631. [CrossRef]
6. National Center for Change Strategy and International Cooperation. Second Biennial Updated Report of the People's Republic of China on Climate Change. 2018-12-12. Available online: <http://tnc.ccchina.org.cn/Detail.aspx?newsId=73251&TId=203> (accessed on 10 November 2022).
7. Zhu, J.C.; Yang, Z.L.; Guo, Y.J.; Zhang, J.K.; Yang, H.K. Short-term load forecasting for electric vehicle charging stations based on deep learning approaches. *Appl. Sci.* **2019**, *9*, 1723. [CrossRef]
8. Dinesh, H.; Pearce, J.M. The potential of agrivoltaic systems. *Renew. Sustain. Energy Rev.* **2016**, *54*, 299–308. [CrossRef]
9. Yang, F.; Niu, T.X.; Zhang, Z.S.; Li, P.; Cao, Y.X.; Zhao, Y.; Li, Y.J. Wind-sand activity characteristics and its influence factors in photovoltaic power station in sand area. *Northwest Hydropower* **2022**, *5*, 79–84+115.
10. Hemming, S.; de Zwart, F.; Elings, A.; Righini, I.; Petropoulou, A. Remote control of greenhouse vegetable production with artificial intelligence—Greenhouse climate, irrigation, and crop production. *Sensors* **2019**, *19*, 1807. [CrossRef]
11. Contreras, J.I.; Baeza, R.; Alonso, F.; Cánovas, G.; Gavilán, P.; Lozano, D. Effect of distribution uniformity and fertigation volume on the bio-productivity of the greenhouse zucchini crop. *Water* **2020**, *12*, 2183. [CrossRef]
12. Xue, J.L. Economic assessment of photovoltaic greenhouses in China. *J. Renew. Sustain. Energy* **2017**, *9*, 033502. [CrossRef]
13. Abdel-Hakim, A.E.; Abo-Elyousr, F.K. Heuristic greedy scheduling of electric vehicles in vehicle-to-grid microgrid owned aggregators. *Sensors* **2022**, *22*, 2408. [CrossRef] [PubMed]
14. Zhang, Q.; Deng, X.S.; Yue, H.Z.; Sun, T.; Liu, Z.Q. Coordinated optimization strategy of electric vehicle cluster participating in energy and frequency regulation markets considering battery lifetime degradation. *Trans. China Electrotech. Soc.* **2022**, *37*, 72–81.
15. Yang, Y.H.; Pei, W.; Deng, W.; Shen, Z.Q.; Qi, Z.P.; Zhou, M. Day-ahead scheduling optimization for microgrid with battery life model. *Trans. China Electrotech. Soc.* **2015**, *30*, 172–180.
16. Lu, X.Y.; Liu, N.; Chen, Z.; Zhang, J.H.; Xiao, X.N. Multi-objective optimal scheduling for PV-assisted charging station of electric vehicles. *Trans. China Electrotech. Soc.* **2014**, *29*, 46–56.
17. Madahi, S.S.K.; Kamrani, A.S.; Nafisi, H. Overarching sustainable energy management of PV integrated EV parking lots in reconfigurable microgrids using generative adversarial networks. *IEEE Trans. Intell. Transp. Syst.* **2022**, *23*, 19258–19271. [CrossRef]
18. Aluisio, B.; Bruno, S.; De Bellis, L.; Dicorato, M.; Forte, G.; Trovato, M. DC-microgrid operation planning for an electric vehicle supply infrastructure. *Appl. Sci.* **2019**, *9*, 2687. [CrossRef]
19. Bhattar, C.L.; Chaudhari, M.A. Centralized Energy management scheme for grid connected DC microgrid. *IEEE Syst. J.* **2023**, *in press*. [CrossRef]
20. El-Taweel, N.A.; Farag, H.; Shaaban, M.F.; AlSharidah, M.E. Optimization model for EV charging stations with PV farm transactive energy. *IEEE Trans. Ind. Inform.* **2022**, *18*, 4608–4621. [CrossRef]
21. Li, Y.Z.; Cai, Y.H.; Zhao, T.Y.; Liu, Y.; Wang, J.; Wu, L.; Zhao, Y. Multi-objective optimal operation of centralized battery swap charging system with photovoltaic. *J. Mod. Power Syst. Clean Energy* **2022**, *10*, 149–162. [CrossRef]
22. Mohammad, A.N.M.; Radzi, M.A.M.; Azis, N.; Shafie, S.; Zainuri, M.A.A.M. An enhanced adaptive perturb and observe technique for efficient maximum power point tracking under partial shading conditions. *Appl. Sci.* **2020**, *10*, 3912. [CrossRef]
23. Wu, J.A.; Xue, Y.S.; Xie, D.L. Optimization of reserve service capability made by electric vehicle aggregator. *Autom. Electr. Power Syst.* **2019**, *43*, 75–81.
24. Wang, Y.; Yang, Z.L.; Mourshed, M.; Guo, Y.J.; Niu, Q.; Zhu, X.D. Demand side management of plug-in electric vehicles and coordinated unit commitment: A novel parallel competitive swarm optimization method. *Energy Convers. Manag.* **2019**, *196*, 935–949. [CrossRef]
25. Guo, Y.; Zhang, H.B.; Cui, K.; Zhao, J. Life-cycle low carbon simulation of smart distribution network considering power loss. In Proceedings of the 2nd IEEE Conference on Energy Internet and Energy System Integration (EI2), Beijing, China, 20–22 October 2018. [CrossRef]
26. Zhao, Z.X.; Shao, C.F.; Chen, J. Effects of private electric vehicles on carbon emission reduction in China during whole life cycle. *Res. Environ. Sci.* **2021**, *34*, 2076–2085.
27. Wang, Z.C.; Jia, N.; Li, J.H.; Lei, B.Y.; Fu, L.B.; Su, Y.Q.; Zhang, J. Influence factors and sensitivity analysis of electric vehicle emission reduction under different energy grid structures. *Energy Conserv. Technol.* **2020**, *38*, 442–448.
28. Kadowaki, M.; Yano, A.; Ishizu, F.; Tanaka, T.; Noda, S. Effects of greenhouse photovoltaic array shading on Welsh onion growth. *Biosyst. Eng.* **2012**, *111*, 290–297. [CrossRef]
29. Gu, W.J.; Sun, Z.C.; Wei, X.Z.; Dai, H.F. A capacity fading model of lithium-ion battery cycle life based on the kinetics of side reactions for electric vehicle applications. *Electrochim. Acta* **2014**, *133*, 107–116. [CrossRef]
30. Yousefi, S.; Moghaddam, M.P.; Majd, V.J. Optimal real time pricing in an agent-based retail market using a comprehensive demand response model. *Energy* **2011**, *36*, 5716–5727. [CrossRef]

31. Dong, T.T. Study on Energy Management and Battery Life for Extended-Range Electric Vehicle. Ph.D. Thesis, Jilin University, Changchun, China, 2013.
32. Wu, J.A.; Xue, Y.S.; Xie, D.L.; Yue, D.; Wen, F.S.; Zhao, J.H. The evaluation and simulation analysis of electric vehicles' reserve capability. *Autom. Electr. Power Syst.* **2018**, *42*, 101–107.
33. PVsyst–Logiciel Photovoltaïque. Available online: <https://www.pvsyst.com> (accessed on 10 September 2022).
34. Shi, L.; Hou, X.L. Research on optimal tilt angle and spacing of PV power station. *Power Syst. Clean Energy* **2017**, *33*, 109–114.
35. Li, S.H. Life Cycle Assessment and Environmental Benefits Analysis of Electric Vehicles. Ph.D. Thesis, Jilin University, Changchun, China, 2014.
36. Wu, J.A.; Xue, Y.S.; Xie, D.L.; Yue, D.; Xue, F. The joint risk dispatch of electric vehicle in day-ahead electricity energy market and reserve market. *Trans. China Electrotech. Soc.* in press.. **2022**. [[CrossRef](#)]

Disclaimer/Publisher's Note: The statements, opinions and data contained in all publications are solely those of the individual author(s) and contributor(s) and not of MDPI and/or the editor(s). MDPI and/or the editor(s) disclaim responsibility for any injury to people or property resulting from any ideas, methods, instructions or products referred to in the content.